Multiscale Modeling of the Nanomechanics of Microtubule Protofilaments – Supplementary Information

Kelly E. Theisen[1], Artem Zhmurov[2,3], Maycee E. Newberry[1], Valeri Barsegov[2,3], and Ruxandra I. Dima[1*]

[1]*Department of Chemistry, University of Cincinnati, Cincinnati, OH 45221,* [2]*Department of Chemistry, University of Massachusetts, Lowell, MA, 01854,* [3]*Moscow Institute of Physics and Technology, Moscow region, Russia, 141700*

E-mail: Ruxandra.Dima@uc.edu

Phone: +1 513 5563961. Fax: +1 513 5569239

[*]To whom correspondence should be addressed

1. Simulation details

The sets of constrained and tagged positions for the simulations of stretching and bending of the tubulin dimers and microtubule protofilaments are all listed in Table S1. Information about the number of simulation runs for each simulation setup and the pulling speed (v_f) used is given in Table S2. The $y(L)$ values used to calculate the bending rigidity (see **Methods** in main text) is obtained using the difference between the coordinates of one of the pulled residues (see Table S3) in the reference structure (initial state) and in the transient structure.

Full Go approach

In the original SOP model,[1] which we refer to as the Simple-Go (SG) model, the native contacts are pairs of residues whose C_α-atoms are within the cut-off distance R_C=8 Å (Lennard-Jones potential in Eq.(1) from the main text). To characterize the intradimer interactions between the α and β-tubulin monomers when tubulin subunits are part of the PF structure, we adopted the Full-Go (FG) model used in our recent study of synaptotagmin 1.[2] In the SOP-FG model, we took into account all the pairwise interactions between amino acids, for which their heavy atoms are within a given cut-off distance. Specifically, the contacts are residue pairs for which either their C_α-atoms are within 8 Å distance, or heavy atoms of their side-chains are within 5.2 Å distance.[3] This led to 63 backbone-backbone and 46 side-chain to side-chain intradimer contacts, i.e. a total of 109 intradimer contacts for PFs (compared to 92 backbone-backbone contacts in the 1TUB file[4]).

2. Stretching simulations for the tubulin dimer

The values of the critical force and the main unfolding events, which correspond to stretching of the dimer, are summarized in Table S4. Fixing position 253 in the α monomer and applying a pulling force $f(t)$ to position 98 in the N-term domain of the β monomer in the tubulin dimer results in a critical unfolding force of $450pN$ in the force-extension curve (FEC; see magenta curve in Figure S3). This corresponds to the disruption of the intradimer interface upon unfolding of the

α monomer (middle conformation at the bottom of Figure S3). Here, the first transition is the unfolding of the positions 243 (T7 loop) to 262 (loop separating H8 and S7) in the α monomer. This is followed by the unfolding of the regions 202 (S6) to 242 (T7 loop) and 263 (loop next to S7) to 308 (loop next to S8), and then by unraveling of the regions 189 (H5) to 238 (H7) and 268 (S7) to 381 (loop after S10). Finally, at $450pN$ the disruption of the intradimer interface occurs.

Fixing position 326 in the α monomer and pulling position 221 in the middle domain of the β monomer in the dimer also leads to a critical force of $450pN$ (blue curve in Figure S3) and shows unfolding only in the α monomer (last structure on the bottom of Figure S3), but the unfolding pathway is different from the one described above. First, positions 306 (loop between H9 and S8) to 351 (S9) unfold, which is followed by the unraveling of the regions 268 (S7) to 305 (loop separating H9 and S8) and 352 (S9) to 378 (S10). Next, positions 238 (H7) to 267 (S7) unfold and the C-term detaches from the rest of the monomer while losing most of it's helical structure. Finally, the 155 (H4) to 237 (H7) region unfolds, which brings about the disruption of the intradimer interface.

The critical unfolding force resulting from fixing the position 257 in the α monomer and applying force to position 407 in the β monomer is $340pN$ (orange curve in Figure S3). This value is substantially lower than the critical forces for the two pulling geometries described above. This is the only case resulting in the partial unfolding of the β monomer (first structure on the bottom of Figure S3). Our previous results[4,5] indicate that the C-term domain in the β-tubulin can withstand $\sim 150pN$ of force. Therefore, when the C-term domain in the β monomer is stretched, the first transition is the unfolding of positions 385 (H11) to 407 (loop after H11) in the β monomer together with the detachment of the rest of the C-term domain (H12). Next, the following parts in the α-tubulin monomer unfold: positions 245 (T7 loop) to 265 (loop between H8 and S7), positions 214 (H6) to 244 (T7 loop) and 266 (S7) to 287 (M loop). The last unfolding event before the breakage of the interface is unfolding of the α-tubulin, including the residues 192 (H5) to 213 (H6), 287 (M loop) to 311 (loop before S8), and 360 (loop before S10) to 381 (loop after S10). (Note: All of these unfolding pathways persist when the specified β monomer residues are fixed instead, and the α monomer residues are pulled.)

To examine the effect of the pulling speed on the unfolding transitions in the tubulin dimer, we conducted simulations using 5-, 10- and 20-times higher pulling speed v_f=9.5, 19.0, and 38.0$\mu m/s$. The peaks in the resulting FECs become less distinct with increased v_f. Indeed, an applied force destabilizes the near-equilibrium intermediate states formed at the low pulling speed v_f=1.9$\mu m/s$ (Figure S4). For a specific pulling geometry (middle domain in the α monomer with the N-term domain in the β monomer), we observe a new unfolding pathway at a 20-fold higher v_f. Here, the β monomer unfolds almost completely, in addition to unfolding in the α monomer (magenta FEC in Figure S3), under $\sim 400pN$ force. For a different pulling arrangement (middle domain in the α monomer and middle domain in the β monomer), the unfolding pathway changes when a 10-fold higher v_f is used. All the unfolding events are now lumped into two peaks in the corresponding FEC. We also observe unfolding and refolding of a small portion of the β-tubulin. For the last pulling geometry (middle domain in the α monomer with the C-term domain in the β monomer), the unfolding mechanism is very robust, as the unfolding pathway did not change even at the 20-fold faster v_f.

References

(1) Hyeon, C.; Dima, R.; Thirumalai, D. *Structure* **2006**, *14*, 1633–1645.

(2) Duan, L.; Zhmurov, A.; Barsegov, V.; Dima, R. *J. Phys. Chem. B* **2011**, *115*, 10133–10146.

(3) Kolinski, A.; Godzik, A.; Skolnick, J. *J. Chem. Phys.* **1993**, *98*, 7420–7433.

(4) Dima, R.; Joshi, H. *Proc. Natl. Acad. Sci.* **2008**, *105*, 15743–15748.

(5) Joshi, H.; Momin, F.; Haines, K.; Dima, R. *Biophys. J.* **2010**, *98*, 657–666.

(6) Grafmuller, A.; Voth, G. *Structure* **2011**, *19*, 409–417.

Table S 1: Positions in the longitudinal interdimer interface used as constrained/tagged residues.

System	Constrained Positions	Tagged Positions
Tubulin Dimer:		
middle domain α, N-term domain of β	$\alpha-253$	$\beta-98$
middle domain α, middle domain of β	$\alpha-326$	$\beta-221$
middle domain α, C-term domain of β	$\alpha-257$	$\beta-407$
Tubulin Protofilaments:		
plus end bending (pulling 3 resid.)	$\alpha-253,248,257,262,325,326,329,348,349$	$\beta-88,338,420$
plus end bending (pulling 1 resid.)	$\alpha-253,248,257,262,325,326,329,348,349$	$\beta-437$
minus end bending (pulling 3 resid.)	$\beta-98,176,177,180,221,224,225,403,407$	$\alpha-90,338,420$
minus end bending (pulling 1 resid.)	$\beta-98,176,177,180,221,224,225,403,407$	$\alpha-439$

Table S 2: Summary of simulation runs completed for each tubulin dimer/protofilament system.

System	No. of runs	Pulling Speed v_f (μm/s)
Tubulin Dimer:		
1TUB dimer, 253-98	7	1.90
1TUB dimer, 326-221	4	1.90
1TUB dimer, 257-407	3	1.90
1TUB dimer, each orientation	1	9.50
1TUB dimer, each orientation	1	19.0
1TUB dimer, 326-221	1	38.0
1TUB dimer, 257-407	1	38.0
1TUB dimer, 253-98	4	38.0
PF Bending from Plus End:		
Interior (pulling 3 resid.)	10	1.90
C-term (pulling 3 resid.)	20	1.90
C-term (pulling 1 resid.)	10	1.90
PF Bending from Minus End:		
Interior (pulling 3 resid.)	20	1.90
C-term (pull 3 resid.)	10	1.90
C-term (pulling 1 resid.)	10	1.90

Table S 3: Positions used to calculate $y(L)$ (see main text) using results from bending simulations.

System	Residue
Plus end, C-term (pulling 3 resid. in chain F)	F-420
Plus end, C-term (pulling C-term in chain F)	F-437
Plus end, Interior (pulling 3 resid. in chain F)	F-88
Minus end, C-term (pulling 3 resid. in chain G)	G-420
Minus end, C-term (pulling C-term in chain G)	G-439
Minus end, Interior (pulling 3 resid. in chain G)	G-90

Table S 4: Summary of results from pulling simulations for the tubulin dimer.

Geometry	Force (pN)	Unfolding Transitions
$\alpha-253, \beta-98$	450	middle and part of N-term domain in α
$\alpha-326, \beta-221$	450	middle and part of N-term domain in α and C-term detaches
$\alpha-257, \beta-407$	340	C-term domain of β, middle and part of N-term domain of α

Table S 5: Number of backbone contacts in the interdimer interface that break in the main steps for bending in the C-term direction at the plus end (number of backbone contacts per interface in the initial state is 51).

Pathway 1:				
Time (ms)	Main steps	AD	BE	HC
7.3	the most bent structure	10	11	10
12.4	part of HC breaks	13	15	23
16.4	F-70 to 98 unfolds	16	17	18
20.0	HC breaks	13	15	51
Pathway 2:				
Time (ms)	Main steps	AD	BE	HC
6.0	the most bent structure	17	16	16
16.4	part of HC breaks	22	14	17
17.5	HC breaks	18	15	51
Pathway 3:				
Time (ms)	Main steps	AD	BE	HC
9.2	the most bent structure	9	15	15
15.9	part of HC breaks	13	14	21
17.4	F-385 to 420 unfolds	20	22	20
18.0	HC breaks	17	17	51
Pathway 4:				
Time (ms)	Main steps	AD	BE	HC
5.3	the most bent structure	14	10	10
14.3	part of HC breaks	20	11	19
19.2	F-69 to 96 unfolds	19	16	25
19.9	F-394 to 420 unfolds	16	27	29
20.1	HC breaks	15	19	51

Table S 6: Number of contacts in the intradimer interface that break in the main steps for two selected pathways for bending in the C-term direction at the plus end (number of backbone contacts per interface in the initial state is 63).

Pathway 2:					
Time (ms)	Main steps	AB	EF	CD	GH
6.0	the most bent structure	10	5	6	11
16.4	part of HC breaks	5	9	7	8
Pathway 3:					
Time (ms)	Main steps	AB	EF	CD	GH
15.8	part of HC breaks	16	5	9	10
17.4	F-385 to 420 unfolds	16	14	9	8

Table S 7: Number of contacts in the interdimer interface that break in the main steps along Pathway 1 for bending in the C-term direction at the minus end (number of backbone contacts per interface in the initial state is 51).

Pathway 1:				
Time (ms)	Main steps	AD	BE	HC
4.0	the most bent structure	17	7	13
15.7	part of HC breaks, G-325 to 350 unfolds	23	18	30
16.1	F-70 to 98 unfolds	18	17	51

Figure Captions

Figure S1

Computational set-up for the bending simulations of a microtubule protofilament, in which a pulling force is applied to the plus end. Here, nine positions in the α monomer at the minus end (orange spheres) are constrained, and selected residues in the β monomer at the plus end (yellow spheres) are tagged in the direction perpendicular to the main axis of the protofilament toward the axis of the MT cylinder (interior bending geometry) or away from it (outward or C-term bending geometry). The list of tagged positions is summarized in Table S1. The capital letter notation, which helps identify each tubulin chain in the two protofilaments, is shown on top of each monomer. For example, the α-tubulin monomer located at the minus end of the PF tetramer is denoted as *G*, while the β-tubulin monomer located at the plus end of the same PF is denoted as F.

Figure S2

Diagram showing the bending angles θ and γ, and the vectors used to calculate these angles. The interior bending angle θ is same as the one used in Ref.[6] Panel (A): Vectors used to determine the angle θ under small bending; G_{COM} denotes the position of the center of mass of chain G (the α-tubulin at the minus end). Panel (B): Vectors used to determine the angle θ near the opening transition in the interdimer interface. Panel (C): vectors used to determine θ when substantial unfolding occurs in the pulled monomer, before the disruption of the interdimer interface; we used the vectors defined by the C-terminal residue of the pulled monomer and the COM of the monomer, and then, between the adjacent monomer and the rest of the chain. Panels (D) and (E) show a schematic for the calculation of θ and γ, respectively.

Figure S3

Simulation results for pulling the interior tubulin dimer. The upper graph shows the force-extension curves (FECs) for each geometry of the applied force depicted by the arrow in the structures below. Also shown are conformational snapshots corresponding to the transition state for the dimer dissociation right before the disruption of the intradimer interface (encircled force peaks in the FECs) for each pulling geometry.

Figure S4

Simulation results for pulling the interior tubulin dimer at high pulling speed v_f. Shown are the FECs for each v_f and for each pulling geometry: $1.9\mu m/s$ (experimental value used in AFM; red curves), $9.5\mu m/s$ (green curves), $19.0\mu m/s$ (blue curves), and $38.0\mu m/s$ (purple curves).

Figure S5

Simulation results for stretching the PF fragment of 4 dimers, in which nine residues in the α-tubulin at the minus end were constrained and a pulling force was applied to position 96 in the β-tubulin at the plus end of the protofilament. Shown are the FEC (left panel), and the part of the FEC corresponding to strain values up to 0.035 (right panel). The structural snapshot depicts the dissociation of the tubulin dimer at the plus end (bottom panel), which corresponds to the force peak of $\sim 450pN$ in the FEC.

Figure S6

Simulation results for bending the PF tetramer in the C-term direction at the plus end of the PF, when a pulling force was applied to the C-terminal residue in the β-tubulin at the plus end. The top graph shows the FEC for each of the two pathways detected. For each pathway, the structural snapshot on the bottom depicts the onset of dissociation, which corresponds to the circled force peak in the FEC.

Figure S7

Simulation results for bending the PF tetramer in the interior direction at the minus end of the PF, when a pulling force was applied to three residues in the α-tubulin at the minus end. Shown are the FEC for the two bending pathways (top panel), and the configuration of the PF in the transition state, i.e. before dissociation, which corresponds to the circled force peaks observed in the corresponding FEC for each pathway.

Figure S8

Simulation results for bending the PF tetramer in the C-term direction at the minus end of the protofilament, in which a pulling force was applied to the C-terminal residue in the α-tubulin at the minus end. Shown are the FEC for the unique bending pathway (top panel), and the configuration of the protofilament in the transition state, i.e. before dissociation, which corresponds to the last force peak observed in the FEC.

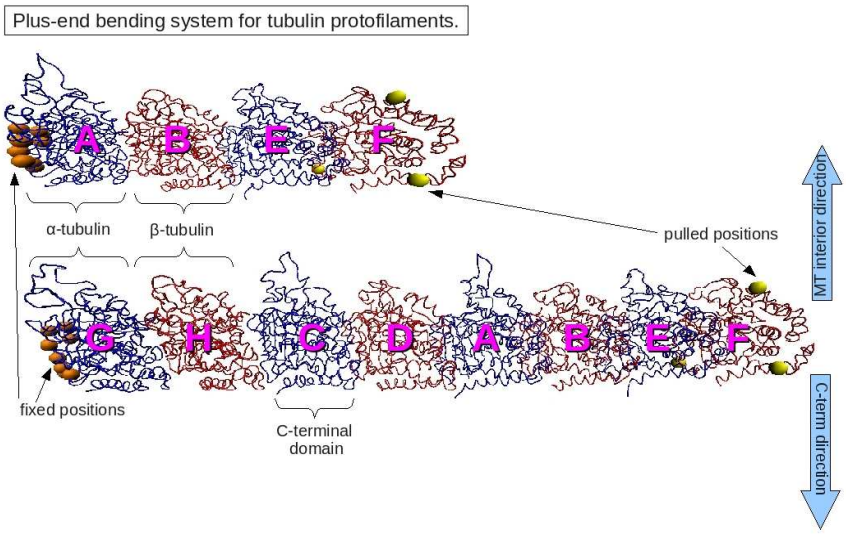

Figure S 1

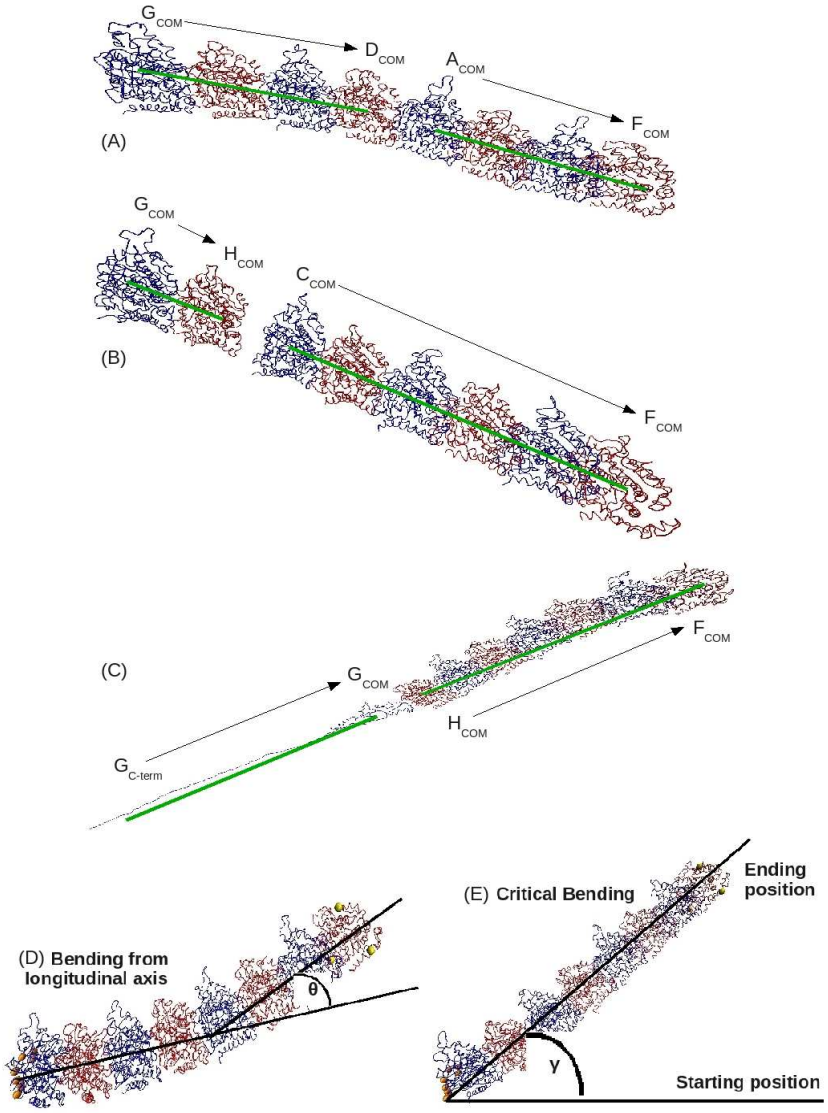
G COM
D COM
A COM
F COM
(A)
G COM
H COM
C COM
F COM
(B)
F COM
(C)
G COM
H COM
G C-term
(D) Bending from longitudinal axis
θ
(E) Critical Bending
Ending position
γ
Starting position

Figure S 2

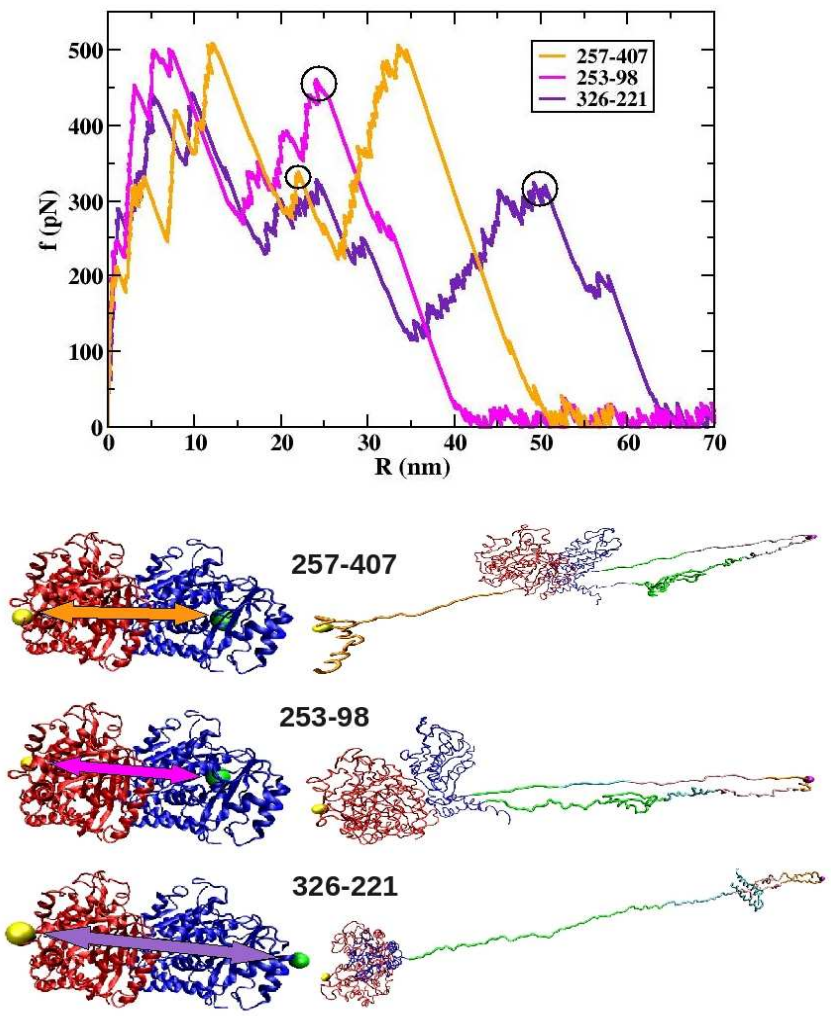

Figure S 3

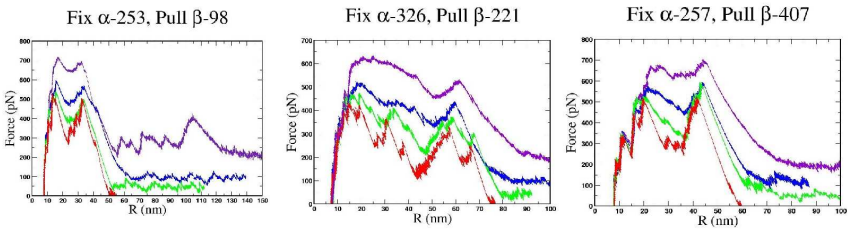

Figure S 4

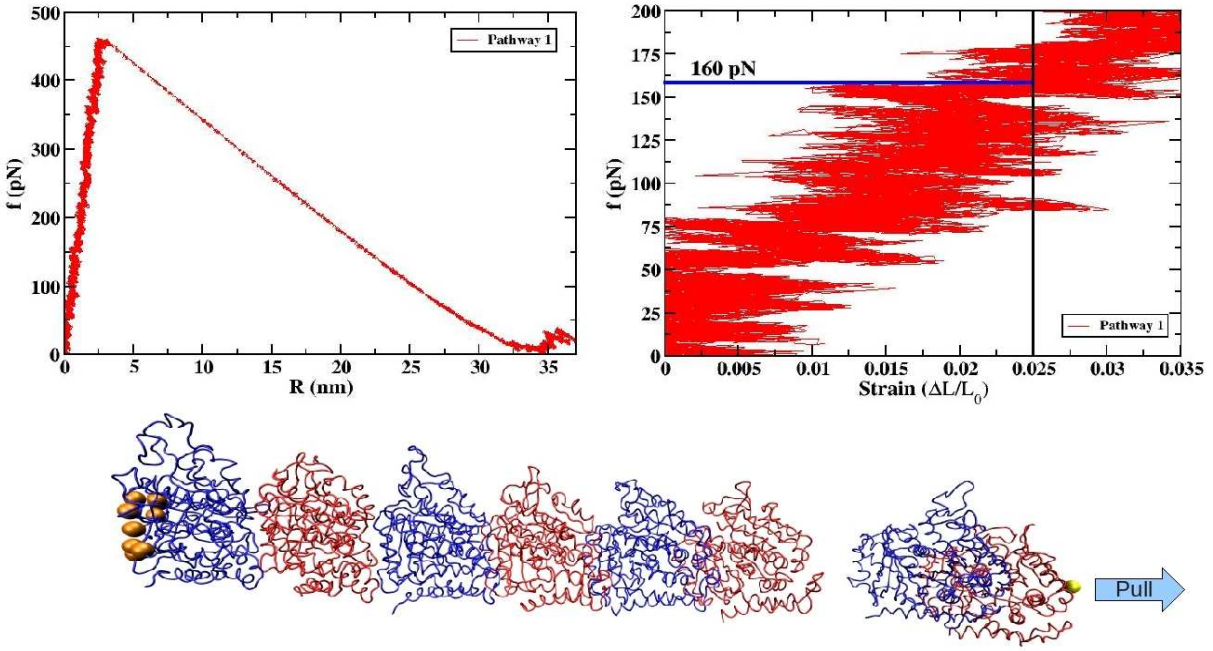

Figure S 5

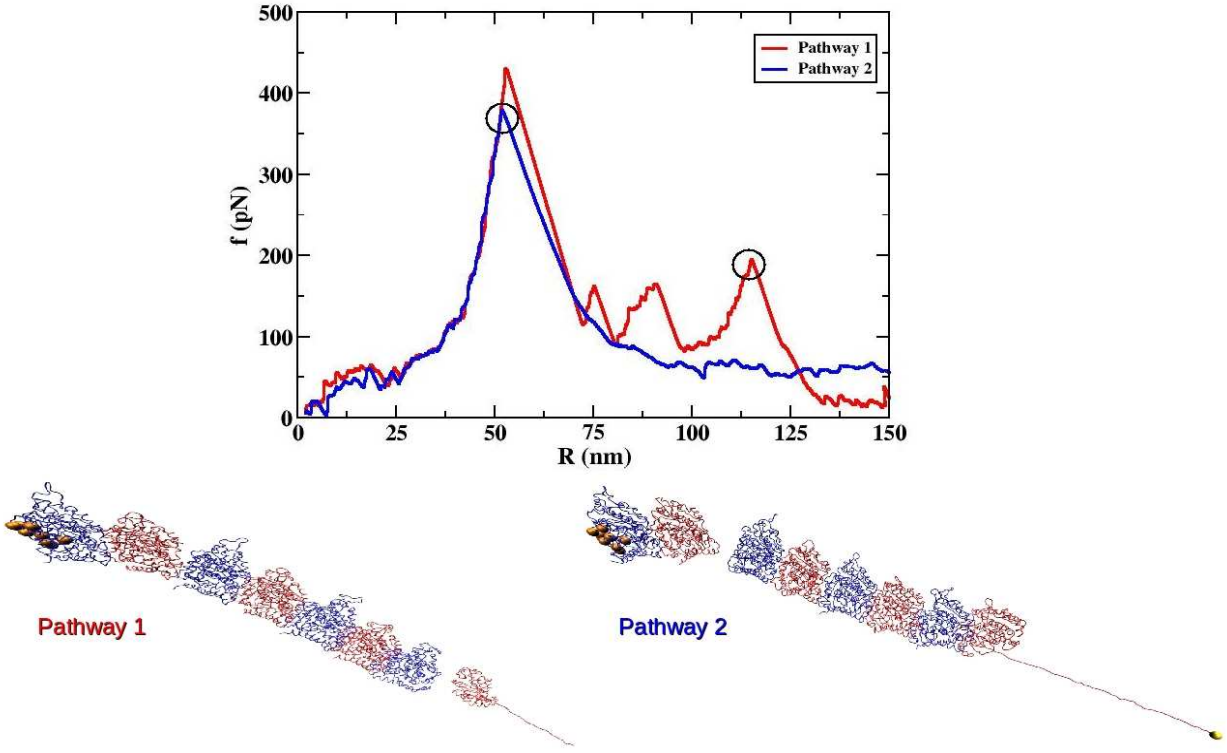

Figure S 6

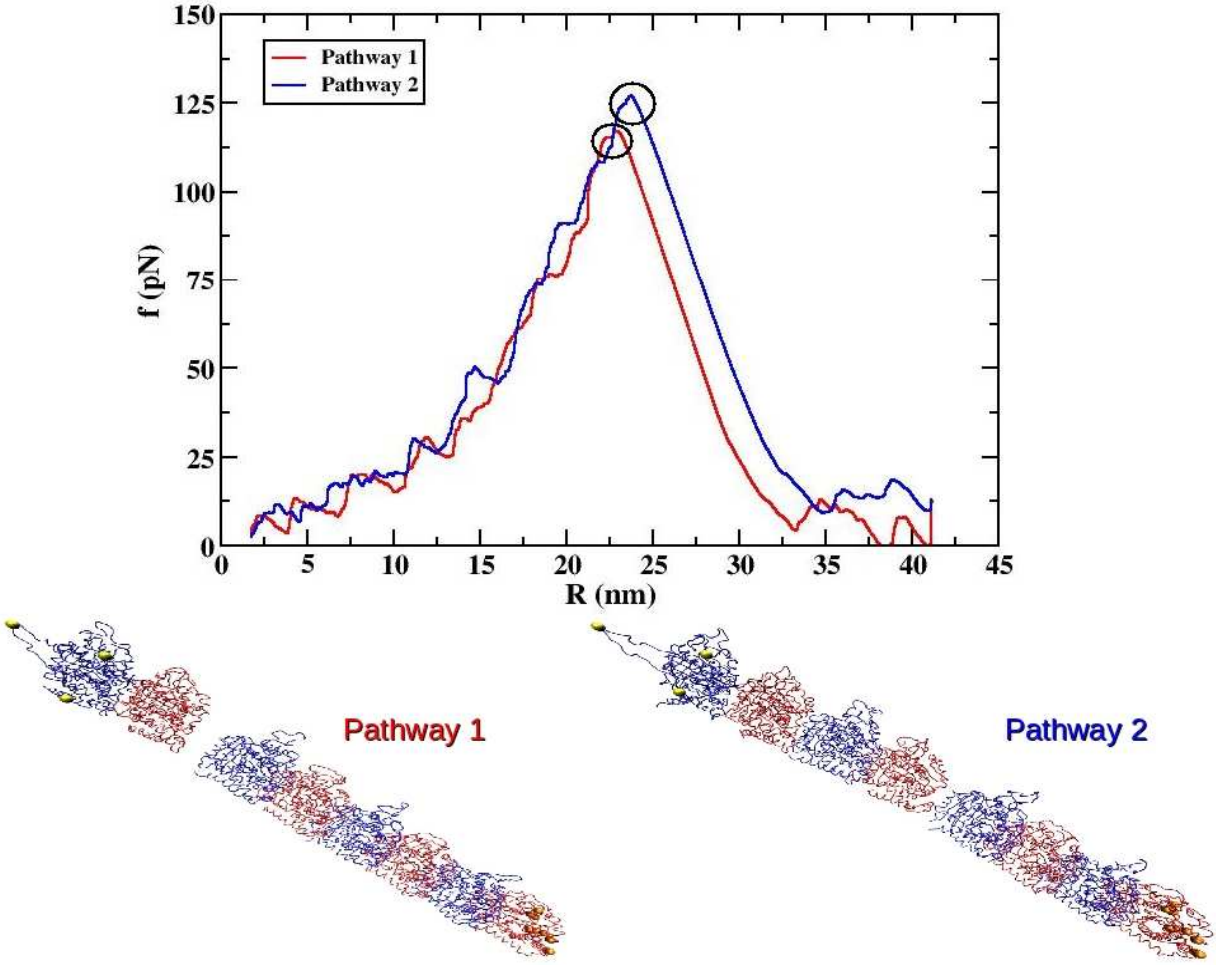
Pathway 1
Pathway 2
f (pN)
R (nm)
0
25
50
75
100
125
150
0
5
10
15
20
25
30
35
40
45
Pathway 1
Pathway 2

Figure S 7

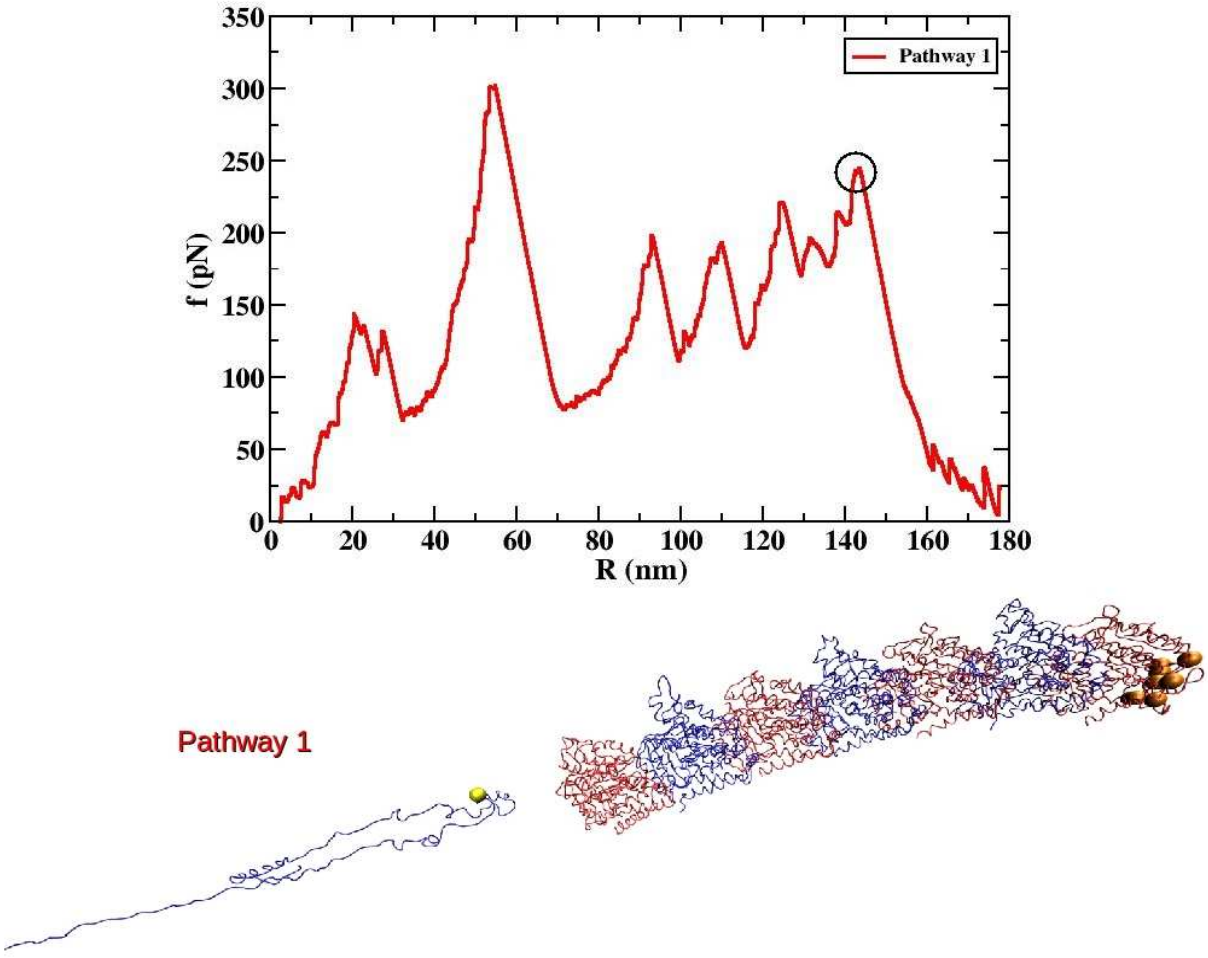
Pathway 1
f (pN)
R (nm)
0
50
100
150
200
250
300
350
0
20
40
60
80
100
120
140
160
180
Pathway 1

Figure S 8